ELSEVIER SCIENCE

Probing the transition from non-localization to localization by K-shell photoemission from isotope-substituted N_2

Daniel Rolles,[a] Markus Braune,[a] Slobodan Cvejanovic,[a] Oliver Geßner,[a] Rainer Hentges,[a] Sanja Korica,[a] Burkhard Langer,[b] Toralf Lischke,[a] Georg Prümper,[a] Axel Reinköster,[a] Jens Viefhaus,[a] Björn Zimmermann,[c] Vince McKoy,[c] and Uwe Becker [a] *

[a] *Fritz-Haber-Institut der Max-Planck-Gesellschaft, 14195 Berlin, Germany*

[b] *Institut für Physikalische Chemie, Universität Würzburg, 97074 Würzburg, Germany*

[c] *California Institute of Technology, Pasadena, CA 91125, USA*

Elsevier use only: Received date here; revised date here; accepted date here

Abstract

The inversion symmetry of a system causes non-local, coherent behaviour of the otherwise localized core holes in homonuclear diatomic molecules such as N_2. This non-locality of the electron emission and the remaining core hole changes in a continuous way into partially localized behaviour if a gradual breakdown of the inversion symmetry is induced by isotope substitution. This is reflected by the loss of interference and the parity mixing of the outgoing photoelectron waves. This is the first experimentally observed isotope effect on the electronic structure of a diatomic molecule.

Keywords: inner-shell photoionization, isotope effect, coherence, core hole localization
PACS: Type your PACS codes here, separated by semicolons ;

1. Introduction

The origin of coherence and delocalization in nature depends on the number of particles involved. In the case of a single particle, the reduction in momentum spread causes delocalized wave-like behavior via Heisenberg's uncertainty relation. All macroscopic double-slit experiments, even the "quantum eraser" (Scully, 1991, Walborn, 2002, 2003), exploit this phenomenon. In many-particle systems, coherence depends on the collectiv freezing of momentum spread which forces the whole system into a joint quantum state where each single particle loses its individuality. The only exception in this context is the two-particle system of identical particles. Here, no momentum spread reduction is required to cause particle coherence, but the intrinsic inversion symmetry of such a system gives rise to a non-localized coherent pair of particles. Homonuclear diatomic molecules are the show-case example for such coherent behavior. The combined effect of inversion symmetry and particle exchange forces all constituents of these molecules to be in a non-local coherent state. Hence, photoemission from these highly localized core electrons can be regarded as a natural molecular two-slit experiment. The coherent core-electron emission in these molecules is supposed to show characteristic interference patterns (Briggs, 2000), particularly in the molecule frame photoelectron angular distributions. However, this coherence is obscured if the two symmetry-adapted gerade and ungerade states are degenerate; the sum of the two resembles exactly the localized emission. In this work, we show the first observation of the coherence of core electrons in N_2 by a

* Corresponding author. Tel.: +49-30-8413-5694; fax: +49-30-8413-5695; e-mail: becker_u@fhi-berlin.mpg.de.

direct measurement of the interference exhibited in their emission.

The transition to the symmetry-broken system of localized electrons is studied by comparing different isotope substituted species of the molecule. Mixed isotope substitution leads to a partial localization of the non-localized core electrons due to the loss of the inversion symmetry by asymmetric vibrations with respect to the inversion center. This is the first observation of a core electron isotope effect. It demonstrates the onset of the transition from non-localization to localization of the core electrons, a phenomenon corresponding to the decoherence process observed in macroscopic two-slit experiments.

With respect to molecular inversion symmetry, the electronic wave functions of homonuclear diatomic molecules can be described as symmetry-adapted linear combinations of the corresponding atomic wave functions Ψ_a and Ψ_b, a situation actually realized by imposition of a fixed phase between them. For the core electrons, these symmetry-adapted wave functions Ψ, called gerade (g) and ungerade (u), can be written as:

$\Psi_g = 1/\sqrt{(2(1+S))}\,[\Psi_a(r) + \Psi_b(r)]$ and

$\Psi_u = 1/\sqrt{(2(1-S))}\,[\Psi_a(r) - \Psi_b(r)]$,

respectively, where the phases of the two orbitals in Ψu differ by π and the overlap-integral is given by $S = \int \Psi_a(r)\Psi_b(r)\,dr$. The corresponding molecular orbitals for K-shell electrons are designated as $1\sigma_g$ and $1\sigma_u$ (Broer, 1999, Kosugi, 2004).

The experimental fingerprint of the coherence of the photoelectron emission from the $1\sigma_g$ and $1\sigma_u$ states in molecular nitrogen is the angular distributions in the molecule frame, which are predicted to exhibit characteristic differences in the angular pattern of the two symmetry states. This refers particularly to their nodal structure, which reflects the angular-momentum-dependent partial wave composition of these electrons. In the non-local coherent case, this composition should be strictly governed by parity selection rules for the gerade and ungerade final core hole states, giving rise to purely odd and even angular momenta in the corresponding partial waves of the $1\sigma_g$ and $1\sigma_u$ photolines.

Here we show that inversion symmetry indeed causes non-local, coherent behaviour of the core electron photoemission from homonuclear diatomic molecules such as N_2. Our results also show that this non-locality changes, in a continuous way, into partially localized behaviour if inversion symmetry violations such as isotope substitution are induced (Rolles, 2005).

2. Experimental

The experiments were performed with vacuum ultraviolet (VUV) synchrotron radiation from beamlines BW3 of HASYLAB at DESY and beamline UE56/2-PGM1 and UE56/1-PGM at BESSY using a set of electron time-of-flight (TOF) spectrometers in combination with an ion time-of-flight spectrometer with a position-sensitive anode. This setup makes it possible to determine all photoelectron and fragment ion momenta in coincidence, yielding, under the axial recoil approximation, the photoelectron angular distribution of fixed-in-space molecules (Heiser, 1997, Becker, 2000). As the N_2:N(1s)-doublet with a splitting of less than 100 meV (Hergenhahn, 2001) had to be resolved while data were acquired over several days, these measurements required extremely high energy resolution of both the beamline (40 meV) and our setup (60 meV) as well as a very high photon beam stability, particularly concerning the energy (10^{-5}). Unresolved spectra would provide the sum of the gerade and ungerade photoemission channels (Weber, 2001, Jahnke, 2002) which, as mentioned above, is insensitive to the localisation character of the core electrons.

3. Results and Discussion

Fig. 1 shows the resolved molecule-frame angular distributions of the $1\sigma_g$ and $1\sigma_u$ photoelectrons, together with the interference angular patterns representing the angular part of the interfering molecular charge distributions. Less characteristic, but still symmetry-specific behaviour occurs also in the non-coincident laboratory-frame angular distribution described by the photoelectron angular distribution parameter β (Yang, 1948) shown in Fig. 2. The distinction is particularly pronounced in the region of the trapped f-wave resonance 9 eV above the N_2:N(1s) threshold because of the dominance of one partial wave in one of the two photoelectron channels only; here the odd f-wave in the gerade channel (Dehmer, 1975, 1976).

We investigated the transition to the symmetry-broken system by comparing the naturally most abundant $^{14,14}N_2$ nitrogen molecule to two different isotopomers, singly substituted $^{14,15}N_2$ and doubly substituted $^{15,15}N_2$ (both 99% purity). Using the electron spectrometer in a non-coincident mode, i.e. without detecting the corresponding fragment ions, we studied the effect of isotope substitution on the photoelectron spectrum. These effects are best illustrated in the *ratio* of the photoelectron spectra of normal and substituted nitrogen: Fig. 3 shows the ratio between the 1s photoelectron spectra of the isotopomer $^{14,15}N_2$ and normal $^{14,14}N_2$ detected at the β-independent "magic angle" θ_m (54.7° with respect to the electric vector of the ionising radiation) where the measured photoelectron intensity is directly proportional to the partial cross section (Yang, 1948) as well as at 0°. The experimental data (purple circles) are shown together with a model calculation of the vibrational effect due to the mass-dependent change of the vibrational constant (dashed black line).

We attribute the additional effects in the cross section and angular distribution to the broken inversion symmetry

in the singly-substituted species leading to a partial localisation of the core hole. While the inversion symmetry of N_2 is preserved in the doubly-substituted species $^{15,15}N_2$, the electron wave function in $^{14,15}N_2$ is slightly modified due to the broken symmetry of the singly-substituted molecule, where the centre of symmetry r_{inv} of the electric charges in the middle of the two atoms no longer coincides with the shifted centre of mass r_{cm} as shown in Fig. 4 (Cacciani, 2000, Bouloufa, 2001). The modified wave functions Ψ' in the molecule with broken inversion symmetry lose their character as parity eigenfunctions and can be described in first order perturbation theory by a linear combination of the original gerade and ungerade wave functions:

$| \Psi'_g > = | \Psi_g > + 1/\Delta E_{g/u} <\Psi_u |H_{asym}|\Psi_g > | \Psi_u >$ respectively

$| \Psi'_u > = | \Psi_u > + 1/\Delta E_{g/u} <\Psi_u |H_{asym}|\Psi_g > | \Psi_g >$,

where $<\Psi_u |H_{asym}|\Psi_g >$ can be understood as an "asymmetry energy" E_{asym} and $\Delta E_{g/u}$ is the g/u energy splitting.

Considering all energy effects caused by isotope substitution, we find that only one, the vibrational motion giving rise to an asymmetry energy of the order of 10 meV (see Fig. 4), is of importance, as all other effects, in particular hyperfine perturbations, which cause g/u symmetry breaking in highly excited states (Pique, 1984, Critchey, 2001), and isotope shifts inducing predissociation in isotopomers (Cacciani, 2000, Bouloufa, 2001), are in the μeV range. The observed effect can therefore be seen as the diatomic analogue of symmetry-breaking by vibronic coupling in triatomic molecules (Domcke, 1977). Comparing this asymmetric part of the vibrational motion in the range of 10 meV with the g/u splitting of $/\Delta E_{g/u} = 100$ meV yields a g/u mixing coefficient $E_{asym}/\Delta E_{g/u}$ of 10%. To obtain the resulting relative change of the intensities, i.e. $<\Psi_g |\Psi_g >/<\Psi'_g |\Psi'_g >$ respectively $<\Psi_u |\Psi_u >/<\Psi'_u |\Psi'_u >$, in first approximation, the square of the mixing coefficient must be multiplied by the normalized intensity difference of the gerade and ungerade channels $(I_g-I_u)/(I_g+I_u)$. At the photon energy considered here, this results in an estimated relative change of the cross section of the order of 1%, which is consistent with the size of the experimentally observed cross-section effect (Fig. 3(c)). The angle-dependent effect is enlarged due to the role of the phase shift between the partial photoelectron waves coming into play for all other emission directions besides the magic angle.

4. Summary and Outlook

Symmetry-breaking through isotope substitution leads to a *partial localization* of the core hole on individual atomic sites, giving rise to *partial coherence* of the outgoing photoelectron waves. This is analog to the *partial "which-way"* information in macroscopic two-slit experiments (Hackermüller, 2004). The continuous nature of the transition makes it possible to control the character of a quantum state being either local or non-local by applying distinct *symmetry violations*, a situation may be also faced by other systems such as *double quantum dots* (Bayer, 2001, Hayashi, 2003). Time-resolved experiments will make it possible to follow the transition from *coherent non-localized* to *uncoherent localized* emission patterns in *core-electron photoemission* of triatomic molecules with two identical atoms.

5. Acknowledgements

The authors acknowledge the essential contributions of R. Diéz Muiño, F.J. García de Abajo, C.S Fadley and M.A. Van Hove to the MSNSP calculations shown in Fig. 1 and along with Jan Bozek many insightful discussion about core-hole delocalisation and coherent photoelectron emission in homonuclear molecules. The help of R. Püttner and F. Gelmukhanov in the interpretation of the effect of isotope substitution on the vibrational structure and the Franck-Condon factors is also greatly acknowledged.

6. References

Bayer, M. *et al.*, 2001. Coupling and Entangling of Quantum States in Quantum Dot Molecules. *Science* **291**, 451–453.

Becker, U., 2000. Angle-resolved electron–electron and electron–ion coincidence spectroscopy: new tools for photoionization studies. *J. Electr. Spectrosc. Relat. Phenom.* **112**, 47–65.

Bouloufa, N. *et al.*, 2001. Predissociation induced by ungerade-gerade symmetry breaking in the $B^1\Pi_u$ state of the $^6Li^7Li$ molecule. *Phys. Rev. A* **63**, 042507.

Briggs, J.S., Walter, M., 2000. Oscillatory structure of Molecular Photoionisation Cross-Sections. *Physics Essays* **13**, 297–302.

Broer, R., Nieuwpoort, W.C., 1999. Hole localization and symmetry breaking. *J. Mol. Structure (Theochem)* **458**, 19–25 and references therein.

Cacciani, P., Kokoouline, V., 2000. Predissociation Induced by Ungerade-Gerade Symmetry Breaking in $^6Li^7Li$ Molecule. *Phys. Rev. Lett.* **84**, 5296–5299.

Critchley, A.D.J., Hughes, A.N., McNab, I.R., 2001. Direct Measurement of a Pure Rotation Transition in H_2. *Phys. Rev. Lett.* **86**, 1725–1728.

Dehmer, J.L., Dill, D., 1975. Shape Resonances in K-Shell Photoionization of Diatomic Molecules. *Phys. Rev. Lett.* **35**, 213–215.

Dehmer, J.L., Dill, D., 1976. Molecular effects on inner-shell photoabsorption. K-shell spectrum of N_2. *J. Chem. Phys.* **65**, 5327–5334.

Diéz Muiño, R., Rolles, D., García de Abajo, F.J., Fadley, C.S., Van Hove, M.A., 2002. Angular distributions of electrons photoemitted from core levels of oriented diatomic molecules: multiplescattering theory in non-spherical potentials. *J. Phys. B* **35**, L359–L365.

Domcke, W., Cederbaum, L.S., 1977. Vibronic coupling and symmetry breaking in core electron ionization. *Chem. Phys*. **25**, 189–196.

Hackermüller, L., Hornberger, K., Brezger, B., Zeilinger, A., Arndt, M., 2004. Decoherence of matter waves by thermal emission of radiation. *Nature* **427**, 711–714.

Hayashi, T., Fujisawa, T, Cheong, H.D., Jeong, Y.H., Hirayama, Y., 2003. Coherent Manipulation of Electronic States in a Double Quantum Dot. *Phys. Rev. Lett.* **91**, 226804.

Heiser, F. *et al.*, 1997. Demonstration of Strong Forward-Backward Asymmetry in the C1s Photoelectron Angular Distribution from Oriented CO Molecules. *Phys. Rev. Lett*. **79**, 2435–2437.

Hergenhahn, U., Kugeler, O., Rüdel, A., Rennie, E.E., Bradshaw, A.M. 2001. Symmetry-Selective Observation of the N 1s Shape Resonance in N_2. *J. Phys. Chem. A* **105**, 5704–5708.

Jahnke, T. *et al., 2002*. Circular Dichroism in K-shell Ionization from Fixed-in-Space CO and N2 Molecules, *Phys. Rev. Lett.* **88**, 073002.

Kosugi, N., 2004. Spin–orbit and exchange interactions in molecular inner shell spectroscopy. *J. Electr. Spectrosc. Relat. Phenom.* **137-140**, 335–343.

Pique, J.P., Hartmann, F., Bacis, R., Churassy, S., Koffend, J.B., 1984. Hyperfine-Induced Ungerade-Gerade Symmetry Breaking in a Homonuclear Diatomic Molecule near a Dissociation Limit: $^{127}I_2$ at the $^2P_{3/2}$-$^2P_{3/2}$ Limit. *Phys. Rev. Lett*. **52**, 267–270.

Rolles, D. *et al.*, 2005, Isotope-induced partial localization of core electrons in the homonuclear molecule N_2, *Nature* **437**, 711–715.

Scully, M.O., Englert, B.G., Walther, H., 1991. Quantum optical tests of complementarity. *Nature* **351**, 111-116.

Stener, M., Fronzoni, G., Decleva, P., 2002. Time dependent density functional study of the symmetry resolved N 1s photoionization in N_2. *Chem. Phys. Lett*. **351**, 469–474.

Walborn, S.P., Terra Cunha, M.O., Pádua, S., Monken, C.H., 2002. Double-slit quantum eraser. *Phys. Rev A* **65**, 033818.

Walborn, S.P., Terra Cunha, M.O., Pádua, S., Monken, C.H., 2003. Quantum Erasure. *American Scientist* **91**, No. 4, p. 336.

Weber, Th. *et al*., 2001. K-shell photoionization of CO and N_2: is there a link between the photoelectron angular distribution and the molecular decay dynamics? *J. Phys. B* **34**, 3669–3678.

Yang, C.N., 1948. On the Angular Distribution in Nuclear Reactions and Coincidence Measurements. *Phys. Rev*. **74**, 764–772.

Zimmermann, B., Wang, K., McKoy, V., 2003. Circular dichroism in K-shell ionization from fixed-in-space CO and N_2. *Phys. Rev. A* **67**, 042711.

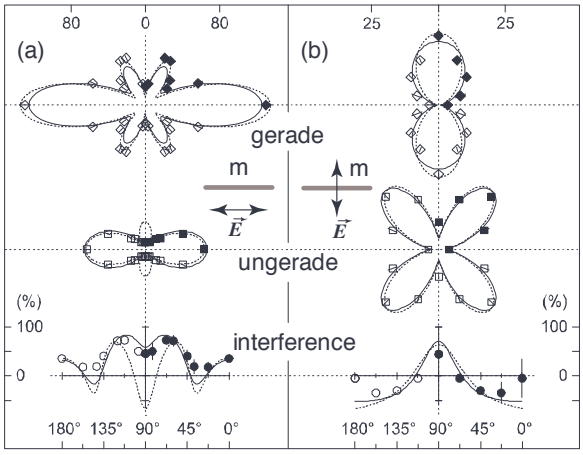

Fig. 1: Molecule frame photoelectron angular distributions (MPAD's) for the gerade (upper panel) and ungerade (middle panel) N(1s) core photoelectron emission of N_2 at a photon energy of hν = 419 eV measured in the plane perpendicular to the light propagation direction for molecules oriented parallel (a) and perpendicular (b) to the light polarisation vector through selection by an ion momentum resolving imaging detector. The fractional interference angular pattern shown in the lower panel of the figure are the differences between the g and u MPAD's divided by their respective sums (g-u)/(g+u). The open symbols are the mirror images of the measured data points (full diamonds, squares, and circles, respectively) which are obtained by a least-squares fit of the coincident spectra. The error bars reflect the statistical uncertainty of the fit. The solid lines represent calculations in the partially relaxed core Hartree-Fock (RCHF) approximation (Zimmermann, 2003), the dotted lines are predictions for non-local, coherent electron emission calculated in the Multiple Scattering in Non-Spherical Potentials (MSNSP) approach (Diez Muino, 2002). All angular pattern data are presented on a relative scale in arbitrary units shown at the upper margin, but unscaled with respect to each other.

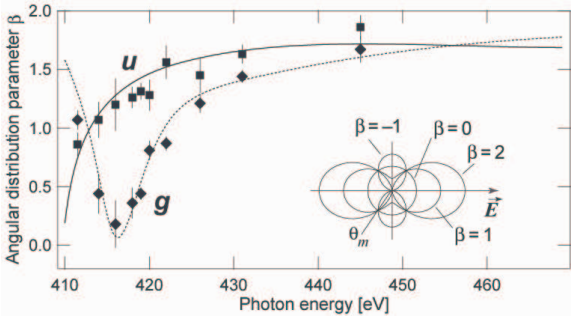

Fig. 2: Photoelectron angular distribution parameter β for N_2:N(1s) electron emission in the range from 410 eV to 450 eV photon energy. The symbols represent the experimental data for the gerade (diamonds) and ungerade (squares) state. The error bars reflect the statistical and calibrational error. The results are compared to calculations in the partially relaxed core Hartree-Fock (RCHF) approximation.

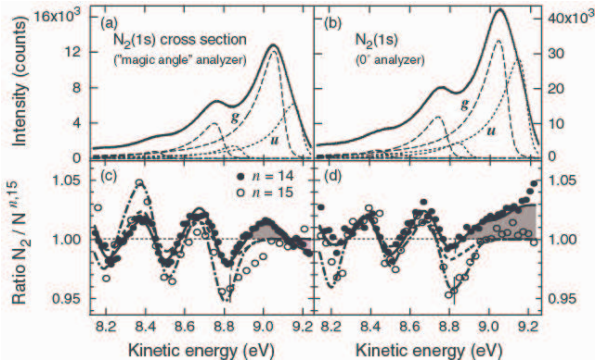

Fig. 3: Isotope effect on N_2. *Top panels*: High-resolution photoelectron spectrum of $^{14,14}N_2$ recorded at a photon energy of hν = 419 eV at the β-independent "magic angle" θ_m (left) and at 0° with respect to the polarisation vector of the ionising radiation (right). The measured spectrum (solid line) in the range of the 1s photoline is shown together with a least-squares fit of its two symmetry-components gerade (dashed line) and ungerade (dotted line) and their respective vibrational progression up to the third vibrational level. *Bottom panels*: Spectral ratio $^{14,14}N_2/^{14,15}N_2$ (full circles) compared to $^{14,14}N_2/^{15,15}N_2$ (open circles) for the same angles as above. The solid lines are model calculations which include the vibrational effect and, for $^{14,15}N_2$, also the cross section effect due to symmetry breaking. For the latter, the dashed line shows a model calculation of the vibrational effect only.

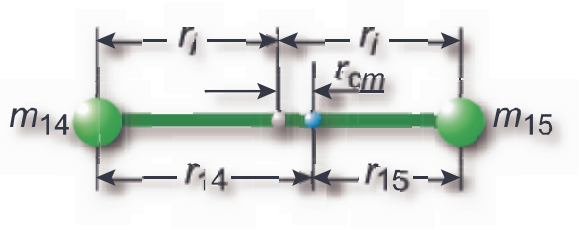

$$r_{cm} = \frac{m_{15}r_i - m_{14}r_i}{m_{15} + m_{14}} = \frac{1}{29} \cdot r_i \Rightarrow \frac{r_s}{r_i} = 0.0345$$

Fig. 4: Shifted center of mass r_{cm} in isotope substituted $^{14,15}N_2$ relative to the geometric center r_i.